

1 **Tandem mass spectrum similarity-based network analysis using ¹³C-labeled and**
2 **non-labeled metabolome data to identify the biosynthesis pathway of the blood**
3 **pressure-lowering asparagus metabolite asparaptine A**

4

5 Ryo Nakabayashi^{1,*}, Yutaka Yamada¹, Tomoko Nishizawa¹, Tetsuya Mori¹, Takashi Asano²,
6 Masanari Kuwabara³, Kazuki Saito¹

7

8 1 RIKEN Center for Sustainable Resource Science, Yokohama 230-0045, Japan

9 2 Iwate Medical University, Iwate 028-3694, Japan

10 3 Toranomon Hospital, Tokyo 105-8470, Japan

11

12 **Abstract**

13 Asparaptine, a conjugate of arginine and asparagusic acid, was found in asparagus (*Asparagus*
14 *officinalis*) as a naturally occurring inhibitor of angiotensin-converting enzyme (ACE) *in vitro*.
15 The biosynthetic pathway to asparaptine is largely unknown; however, it is suggested that
16 asparagusic acid may be biosynthesized from valine. To determine which metabolites are
17 involved in the asparaptine biosynthetic pathway, we performed tandem mass spectrometry
18 similarity-based metabolome network analysis using ¹³C labeled and non-labeled valine-fed
19 asparagus calluses. We determined that valine is used as a starting material,
20 *S*-(2-carboxy-*n*-propyl)-cysteine as an intermediate, and two new metabolites as asparaptine
21 analogs, lysine- and histidine-type conjugates, are involved in the pathway. Asparaptine was
22 therefore renamed asparaptine A (arginine type), and the two analogs were named
23 asparaptines B (lysine type) and C (histidine type). Oral feeding of asparaptine A to a
24 hypertensive mouse species showed that this metabolite lowers both blood pressure and heart
25 rate within two hours and both of which were back to normal two days later. These results
26 suggest that asparaptine A may not only have effects as an ACE inhibitor, but also has
27 β-antagonistic effects, which are well-known to be preventive for cardiovascular diseases.

28 Introduction

29 Stable isotope labeling is a powerful approach in metabolomics for determining the number of
30 elements in detected metabolites using liquid chromatography-tandem mass spectrometry
31 (LC-MS/MS)¹. LC-MS/MS analysis is useful for narrowing down metabolite identities using
32 peak resolution and mass accuracy², but it is difficult to determine unambiguous molecular
33 formula. A metabolite labeled with stable isotope (¹³C, ¹⁵N, ¹⁸O, or ³⁴S) and its non-labeled
34 counterpart are typically detected at almost the same retention time and can be paired. The
35 shifted mass to charge (m/z) value between metabolite pairs allows the numbers of C, N, O, or
36 S to be determined with an established procedure in plants³⁻⁹. Recently, principal component
37 analysis (PCA) was used for pairing fully ¹⁵N-labeled and non-labeled metabolites to
38 characterize the missing monoterpene indole alkaloids in *Catharanthus roseus*¹⁰. The PCA
39 clearly separated types of metabolites that differed significantly between samples. In that
40 study, pairing was manually performed using coordinates of loading factors in the PCA as
41 well as retention times and m/z values of the precursor ions. Manual pairing approaches are
42 suitable for chemical assignments of dozens of metabolites with the caveat of requiring long
43 data analysis time; however, are unfeasible for assignments of metabolome that can include
44 hundreds of metabolites.

45
46 To streamline the processes involved, it is essential to apply methods of computational
47 automation. For instance, molecular networking by Global Natural Product Society^{11,12} or
48 MS-DIAL/FINDER^{3,13} programs enable the creation of MS/MS similarity-based networks
49 that can assist structural analog characterization. Theoretically, the fragmentation “pattern” of
50 isotope-labeled and non-labeled metabolites should be almost identical since the chemical
51 properties of the metabolites, apart from their m/z value, are otherwise the same. It is possible
52 to pair stable isotope-labeled and non-labeled MS/MS spectra by using MS/MS similarity
53 scores in addition to retention times and m/z values.

54
55 Asparaptine, which consists of arginine and asparagusic acid, is a naturally occurring inhibitor
56 of angiotensin-converting enzyme (ACE) in asparagus (*Asparagus officinalis*)¹⁴. It has been
57 suggested that the asparagusic moiety of asparaptine is biosynthesized from valine¹⁵; however,
58 the biosynthetic pathway to asparagusic acid and asparaptine remains largely unknown. In this
59 study, we performed MS/MS spectrum similarity-based network analysis using ¹³C-labeled
60 and non-labeled metabolome data to determine metabolites involved in the biosynthetic
61 pathway of asparaptine. We showed that valine is a starting material for the biosynthesis of
62 asparaptine and that *S*-(2-carboxy-*n*-propyl)-L-cysteine is an intermediate of the pathway.
63 Moreover, we found two new structural analogs of asparaptine: conjugates of lysine/histidine
64 and asparagusic acid. Thus, asparaptine was renamed as asparaptine A, and the lysine- and
65 histidine-type conjugates were named as asparaptine B and C, respectively. Finally, we

66 characterized that asparaptine A lowers blood pressure and heart rate of a hypertensive mouse
67 species.

68

69 **Experimental Section**

70 **Plant materials**

71 Calluses derived from green asparagus (*Asparagus officinalis*)¹⁶ were used in this study.

72

73 **Chemicals**

74 The following ¹³C amino acids and non-labeled amino acids were used in the study: L-valine
75 (¹³C₅, 99%), L-lysine (¹³C₆, 99%), L-histidine (¹³C₆, 97%–99%), and L-glutamine (¹³C₅, 99%),
76 (Cambridge Isotope Laboratories, US); and L-valine, L-lysine, and glutamine (Sigma Aldrich
77 Japan, Tokyo), and L-arginine and L-histidine (FUJIFILM Wako Pure Chemical Corporation,
78 Japan).

79

80 **Stable isotope labeling to the calluses**

81 The medium was prepared for the growth of the calluses as following: Murashige Skoog salt
82 (1.38 g) and vitamin (1000×, 300 μL), sucrose (9 g), 1-naphthaleneacetic acid, and kinetin (5
83 μM final concentration), and gelrite (0.2%) in water (300 mL). The pH was adjusted to 5.7
84 with KOH. The solution was then autoclaved for 15 min at 121°C.

85

86 A medium aqa. solution was autoclaved (3 mL) and added to a well of a 6-well plate (BMBio,
87 Japan). Then, 30 μL of 100 mM aqa. solution of ¹³C-labeled amino acid and its non-labeled
88 counterpart were filtered for sterilization, followed by the addition to the medium to achieve a
89 final concentration of 1 mM. A piece of the callus (5-by-5 mm size) was placed in the center
90 of the well. The plate was incubated at 23°C in a dark growth chamber. The medium was
91 refreshed once a month. Calluses were harvested after four months. Three biological
92 replicates were prepared for all samples.

93

94 **Metabolite extraction and untargeted LC-MS/MS analysis**

95 Freeze-dried samples were extracted and analyzed as described in the previous study³.

96

97 **S-plot analysis**

98 SIMCA-P (v 12.0.1) was used in this study. Pareto scaling was applied with the default
99 parameters.

100

101 **Data processing for metabolome network analysis**

102 Data matrix was created using MassLyncs 4.2. In preliminary processing for metabolome
103 network analysis, isotopic ions in regions (monoisotopic ions (M) + 1.0034/2.0068 ± 0.01 Da)

104 were removed to simplify MS/MS spectra in ¹³C-labeled and non-labeled data. The scores of
105 MS/MS similarity by dot products were calculated for the simplified ¹³C-labeled and
106 non-labeled MS/MS spectra under the following conditions: retention time ± 0.05 ; difference
107 of m/z value on precursor ion, $0 \leq n \leq 5$; number of product ion ≥ 3 . The calculation was
108 performed according to the previous study³. Nodes representing ions were clustered using the
109 spinglass method in R (https://igraph.org/r/doc/cluster_spinglass.html). The parameters on
110 gamma and spins were changed to 1.5 and 200, respectively. The information of nodes and
111 edges on the metabolome network analysis is available at DROP Met
112 (http://prime.psc.riken.jp/menta.cgi/prime/drop_index). Metabolome networks using the
113 similarity scores obtained by dot products were visualized using the PlaSMA database
114 (<http://plasma.riken.jp/>).

115

116 **Orally feeding hypertensive mice with asparaptine A**

117 Experiments were outsourced to a company (UNITECH Co., Ltd., Japan). These experiments
118 were conducted in accordance with the regulations of the Act on Welfare and Management of
119 Animals, the Standards relating to the Care and Keeping and Reducing Pain of Laboratory
120 Animals, the Basic Guidelines of the Ministry of Education, Culture, Sports, Science and
121 Technology, the Guidelines for Proper Conduct of Animal Experiments, and the Standards
122 relating to the Methods of Destruction of Animals. In addition, the implementation of this
123 study has been approved by the Animal Experiment Committee of UNITEC Corporation
124 (AGR RK-171011-100).

125

126 A total of 14 mice (hRN8-12 \times hAG2-5, F1 generation) were moved from a rearing place to a
127 site for measuring their blood pressure. The animals were reared for 6–8 weeks for adaptation
128 to the following conditions: room temperature 22°C–26°C; humidity 40%–65%; light 8:00
129 AM–20:00 PM, cage, each per mouse; cage exchange or cleanup, every week; and feed and
130 water, discretionary. Asparaptine aqa. solution (2.5 mg/mL) was orally fed to seven mice (age:
131 15–16 weeks) for 50 μ g/g body weight, and water was fed to another seven mice as a control
132 group. Blood pressure was measured by the tail-cuff method at one, two, and three hours and
133 two days after feeding.

134

135 **Results and Discussion**

136 The biosynthetic pathway of asparaptine (called asparaptine A hereafter) is largely unknown;
137 however, it has been suggested that the asparagusyl moiety of asparaptine A may be
138 biosynthesized from the amino acid valine. A few steps from valine were only revealed with
139 radio isotope labeling¹⁵. To understand whether valine can be used as a starting material for
140 the asparagusyl moiety, stable isotope labeling was performed [**Supporting Information (SI)**
141 **Figure S1**]. Since asparagus is a perennial plant, this makes it difficult to use the asparagus

142 plant itself for stable isotope labeling. In this study, a callus line derived from green
143 asparagus¹⁶ was used instead.

144

145 To increase the labeling rate, pieces of asparagus callus were grown for four months in
146 medium containing ¹³C-labeled or non-labeled valine, which were then harvested for
147 untargeted analysis. Comprehensive data acquisition was performed using liquid
148 chromatography-tandem mass spectrometry (LC-MS/MS). All scanned MS/MS data were
149 then output using MassLyncs. To evaluate the quantity of metabolites that were labeled with
150 ¹³C valine, tracing of endogeneous ¹³C-labeled and non-labeled valine was performed (**Figure**
151 **1**), which indicated that the labeling was successful and the average labeling rate was
152 approximately 60% in three biological samples.

153

154 Using the MS/MS spectra, similarity scores were calculated using dot product method. A
155 metabolome network using both ¹³C-labeled and non-labeled data was created with the
156 following conditions (similarity score ≥ 0.8 ; mass range, m/z 100–500; difference of m/z value
157 on precursor ion $1 \leq n \leq 5$) (**Figure 2; SI Figure S2**). Each node (ion) is represented in a
158 community that consists of other nodes. The communities are constructed when nodes show
159 high similarity scores to each other. In this analysis, the nodes from ¹³C-labeled and
160 non-labeled metabolites were connected with the MS/MS similarity score >0.8 . The
161 community members appeared to derive from one peak, indicating that multi-scanned MS/MS
162 spectra in a metabolite peak were summarized to a single community. Possible intermediates
163 and analogs were searched by their exact mass for $[M + H]^+$. Communities that included
164 nodes of asparaptine, nodes of a possible intermediate, and distinct nodes for two possible
165 asparaptine analogs were detected with their exact mass (**SI Figures S3–8**). In this analysis,
166 asparagusic acid and its glucose ester could not be detected in the samples.

167

168 The incorporation of ¹³C to these metabolites was then evaluated by LC-MS/MS. To
169 determine whether the asparagusyl moiety is derived from valine, comparative analysis of
170 ¹³C-labeled and non-labeled MS/MS spectrum was performed (**Figure 3a**). The ion peak of
171 non-labeled asparaptine A was identified using an authentic standard compound¹⁴. In the
172 ¹³C-labeled MS/MS spectrum, mass-shifted product ions were confirmed. The fragmentation
173 patterns indicated that asparagusyl moiety of asparaptine was derived from valine.
174 Comparative analysis on the possible intermediate was also performed (**Figure 3b**), which
175 showed the exact mass of *S*-(2-carboxy-*n*-propyl)-L-cysteine as $[M + H]^+$. A previous study
176 suggested that the S atom is derived from the attachment of the cysteine moiety¹⁵. The
177 precursor ion observed at m/z 208.0646 was found to be nearly identical to the theoretical one
178 (m/z 208.0644 for $C_7H_{14}NO_4S$ $[M + H]^+$). The fragmentation patterns indicated that the bonds
179 of N and S were cleaved in the cysteine moiety, suggesting that this metabolite is derived

180 from the cysteine derivative.

181

182 We hypothesized that, of the two possible analogs, one may be a conjugate of lysine and
183 asparagusic acid and the other one may be a conjugate of histidine and asparagusic acid (**SI**
184 **Figures S4**). To elucidate their structure, the MS/MS spectrum acquired from calluses labeled
185 with ^{13}C valine and ^{13}C lysine/ ^{13}C histidine were compared for fragmentation analyses
186 (**Figure 4**). The analysis revealed the incorporation of ^{13}C valine to the asparagusic moiety
187 and that of ^{13}C -lysine/ ^{13}C histidine to the lysyl or histidyl moiety. The fragmentation patterns
188 identified the cleavage of amino and carboxyl moieties, showing that the asparagusic moiety
189 is conjugated to the amino moiety at the α position of lysine/histidine. Thus, asparaptine was
190 renamed as asparaptine A. The lysine- and histidine-type analogs were named as asparaptines
191 B and C, respectively. The existence of these analogs suggest that additional asparaptine
192 analogs may also exist in asparagus plants or calluses. A cutting-edge LC-MS/MS instrument
193 with higher sensitivity is expected to detect the additional analogs.

194

195 As mention above, asparaptine A shows the ACE inhibitory activity *in vitro*. Interestingly, the
196 conjugate of proline and asparagusic acid [named asparaptine K in this study (**SI Figure S4**)]
197 has been reported as a blood pressure-lowering agent¹⁷. To confirm blood pressure-lowering
198 effect *in vivo*, hypertensive mice were orally fed with asparaptine A (**Figure 5**). Both the
199 systolic and diastolic blood pressure in the asparaptine A-fed mice remarkably decreased to
200 20 mmHg lower than those in control group in two hours after feeding (**Figures 5a** and **5b**).
201 After two days, the blood pressure completely returned to normal. This observation suggested
202 that asparaptine A has a rapid action in reducing blood pressure. Moreover, the heart rate in
203 the asparaptine A-fed mice significantly decreased in two hours, before recovering quickly
204 (**Figure 5c**). These results suggest that asparaptine A may not only have effects as an ACE
205 inhibitor, but also has β -antagonistic effects. These effects are well-known to be preventive
206 for cardiovascular diseases^{18,19}. Short-acting ACE inhibitors with strong anti-hypertensive
207 effects are useful for patients with aortic dissection or rupture in emergency department.
208 However, most ACE inhibitors are well-known as long-acting anti-hypertensive agents, which
209 makes them difficult to use for patients who require urgent surgical intervention. Asparaptine
210 A may be an important candidate as an anti-hypertensive drug in future medical use due to the
211 strong observed anti-hypertensive effects combined with rapid degradation in the mice.

212

213 **Conclusion**

214 In this study, we performed the MS/MS similarity-based network approach to analyze
215 ^{13}C -labeled and non-labeled metabolome data from asparagus calluses. The analysis
216 characterized metabolite pairs despite differences in the m/z value. Four paired ions were
217 analyzed to determine the structure of an unknown pathway intermediate

218 *S*-(2-carboxy-*n*-propyl)-L-cysteine, asparaptine A, and two previously unidentified analogs
219 asparaptines B and C. This analysis enables the automatic extraction of accurate pairs of ions
220 derived from ¹³C-labeled and non-labeled metabolites in metabolomics data. The analysis is
221 applicable to software programs that require off-the-shelf approaches to pair stable
222 isotope-labeled and non-labeled metabolites.

223 **Associated Contents**

224 **Supporting Information**

225 The Supporting Information is available free of charge at online.

226

227 **Figure S1.** ¹³C labeling of asparagus calluses.

228 **Figure S2.** Parameters of the metabolome network analysis.

229 **Figure S3.** Searched metabolites in the metabolome network analysis.

230 **Figure S4.** Searched possible analogs of asparaptine A.

231 **Figure S5.** Linking nodes (¹³C-labeled) to their counterparts (non-labeled) on asparaptine A.

232 **Figure S6.** Linking nodes (¹³C-labeled) to their counterparts (non-labeled) on
233 *S*-(2-carboxy-*n*-propyl)-L-cysteine.

234 **Figure S7.** Linking nodes (¹³C-labeled) to their counterparts (non-labeled) on asparaptine B.

235 **Figure S8.** Linking nodes (¹³C-labeled) to their counterparts (non-labeled) on asparaptine C.

236

237 **Author Information**

238 **Corresponding Author (*)**

239 Ryo Nakabayashi (ORCID: 0000-0002-8674-0928)

240 RIKEN Center for Sustainable Resource Science, Yokohama 230-0045, Japan

241 Tel: +81-45-503-9442

242 Email: ryo.nakabayashi@riken.jp

243

244 Yutaka Yamada

245 RIKEN Center for Sustainable Resource Science, Yokohama 230-0045, Japan

246

247 Tomoko Nishizawa

248 RIKEN Center for Sustainable Resource Science, Yokohama 230-0045, Japan

249

250 Tetsuya Mori (ORCID: 0000-0001-5347-8890)

251 RIKEN Center for Sustainable Resource Science, Yokohama 230-0045, Japan

252

253 Takashi Asano

254 Iwate Medical University, Iwate 028-3694, Japan

255

256 Masanari Kuwabara (ORCID: 0000-0002-6601-4347)

257 Toranomom Hospital, Tokyo 105-8470, Japan

258

259 Kazuki Saito (ORCID: 0000-0001-6310-5342)

260 RIKEN Center for Sustainable Resource Science, Yokohama 230-0045, Japan

261

262 **Author Contributions**

263 R.N. designed the research. R.N., T.N., and T.A. prepared the callus samples. R.N. and T.M.
264 acquired the metabolome data. R.N. and Y.Y. performed the metabolome network analysis.
265 R.N. analyzed all the data. M.K analyzed the data of blood pressure. R.N. discussed the
266 research with all the co-authors. R.N. wrote the manuscript.

267

268 **Acknowledgments**

269 We would like to thank Hiroshi Tsugawa for technical advices (RIKEN CSRS) and Kouji
270 Takano (RIKEN CSRS) for technical assistance. The hypertensive mice were provided by the
271 RIKEN BRC through the National Bio-Resource Project of the MEXT, Japan.

272

273 **Notes**

274 The authors declare no competing financial interest.

275

276 **References**

- 277 (1) Nakabayashi, R.; Saito, K. *Curr Opin Plant Biol* **2020**, *55*, 84-92.
- 278 (2) Nakabayashi, R.; Sawada, Y.; Yamada, Y.; Suzuki, M.; Hirai, M. Y.; Sakurai, T.; Saito, K.
279 *Anal Chem* **2013**, *85*, 1310-1315.
- 280 (3) Tsugawa, H.; Nakabayashi, R.; Mori, T.; Yamada, Y.; Takahashi, M.; Rai, A.; Sugiyama,
281 R.; Yamamoto, H.; Nakaya, T.; Yamazaki, M.; Kooke, R.; Bac-Molenaar, J. A.; Oztolan-Erol,
282 N.; Keurentjes, J. J. B.; Arita, M.; Saito, K. *Nat Methods* **2019**, *16*, 295-298.
- 283 (4) Nakabayashi, R.; Hashimoto, K.; Toyooka, K.; Saito, K. *Anal Chem* **2017**, *89*, 2698-2703.
- 284 (5) Giavalisco, P.; Li, Y.; Matthes, A.; Eckhardt, A.; Hubberten, H. M.; Hesse, H.; Segu, S.;
285 Hummel, J.; Kohl, K.; Willmitzer, L. *Plant J* **2011**, *68*, 364-376.
- 286 (6) Kera, K.; Fine, D. D.; Wherritt, D. J.; Nagashima, Y.; Shimada, N.; Ara, T.; Ogata, Y.;
287 Sumner, L. W.; Suzuki, H. *Metabolomics* **2018**, *14*, 71.
- 288 (7) Nakabayashi, R.; Tsugawa, H.; Mori, T.; Saito, K. *Metabolomics* **2016**, *12*.
- 289 (8) Glaser, K.; Kanawati, B.; Kubo, T.; Schmitt-Kopplin, P.; Grill, E. *Plant Journal* **2014**, *77*,
290 31-45.
- 291 (9) Wang, Z. Z.; Jones, A. D. *Anal Chem* **2014**, *86*, 10600-10607.
- 292 (10) Nakabayashi, R.; Mori, T.; Takeda, N.; Toyooka, K.; Sudo, H.; Tsugawa, H.; Saito, K.
293 *Anal Chem* **2020**.
- 294 (11) Nothias, L. F.; Petras, D.; Schmid, R.; Duhrkop, K.; Rainer, J.; Sarvepalli, A.; Protsyuk,
295 I.; Ernst, M.; Tsugawa, H.; Fleischauer, M.; Aicheler, F.; Aksenov, A. A.; Alka, O.; Allard, P.
296 M.; Barsch, A.; Cachet, X.; Caraballo-Rodriguez, A. M.; Da Silva, R. R.; Dang, T.; Garg, N.,
297 et al. *Nat Methods* **2020**, *17*, 905-908.
- 298 (12) Kang, K. B.; Ernst, M.; van der Hoof, J. J. J.; da Silva, R. R.; Park, J.; Medema, M. H.;

- 299 Sung, S. H.; Dorrestein, P. C. *Plant J* **2019**, *98*, 1134-1144.
- 300 (13) Tsugawa, H.; Kind, T.; Nakabayashi, R.; Yukihiro, D.; Tanaka, W.; Cajka, T.; Saito, K.;
301 Fiehn, O.; Arita, M. *Analytical Chemistry* **2016**, *88*, 7946-7958.
- 302 (14) Nakabayashi, R.; Yang, Z.; Nishizawa, T.; Mori, T.; Saito, K. *J Nat Prod* **2015**, *78*,
303 1179-1183.
- 304 (15) Mitchell, S. C.; Waring, R. H. *Phytochemistry* **2014**, *97*, 5-10.
- 305 (16) Nakabayashi, R.; Nishizawa, T.; Mori, T.; Sudo, H.; Fujii, I.; Asano, T.; Saito, K. *Plant*
306 *Biotechnol (Tokyo)* **2019**, *36*, 265-267.
- 307 (17) Omura, K. *Kokai-Tokkyo-Koho* **1979**, *Showa54-125669 [in Japanese]*.
- 308 (18) Ponikowski, P.; Voors, A. A.; Anker, S. D.; Bueno, H.; Cleland, J. G. F.; Coats, A. J. S.;
309 Falk, V.; Gonzalez-Juanatey, J. R.; Harjola, V. P.; Jankowska, E. A.; Jessup, M.; Linde, C.;
310 Nihoyannopoulos, P.; Parissis, J. T.; Pieske, B.; Riley, J. P.; Rosano, G. M. C.; Ruilope, L. M.;
311 Ruschitzka, F.; Rutten, F. H., et al. *Eur Heart J* **2016**, *37*, 2129-2200.
- 312 (19) Whelton, P. K.; Carey, R. M.; Aronow, W. S.; Casey, D. E., Jr.; Collins, K. J.; Dennison
313 Himmelfarb, C.; DePalma, S. M.; Gidding, S.; Jamerson, K. A.; Jones, D. W.; MacLaughlin,
314 E. J.; Muntner, P.; Ovbigele, B.; Smith, S. C., Jr.; Spencer, C. C.; Stafford, R. S.; Taler, S. J.;
315 Thomas, R. J.; Williams, K. A., Sr.; Williamson, J. D., et al. *Circulation* **2018**, *138*,
316 e426-e483.

317 **Legends**

318 **Figure 1.** ^{13}C labeling of asparagus calluses.

319 (a) Representative MS spectrum of endogenous valine in ^{13}C -labeled and non-labeled calluses.

320 (b) S-plot using ^{13}C -labeled and non-labeled metabolome data. Differences indicated presence
321 of ^{13}C -labeled and non-labeled valine-derived metabolites. Scale bar, 0.5 cm.

322

323 **Figure 2.** Metabolome network analysis to pair ^{13}C -labeled and non-labeled metabolites.

324 The metabolome network was created with the following conditions (similarity score ≥ 0.8 ;

325 mass range m/z 100–500; difference of m/z value on precursor ion $1 \leq n \leq 5$). Each node

326 indicates a community that consists of nodes (ions), and the edge indicates a similarity score.

327 When nodes have high density, communities were created. When a node in a community

328 share a similarity score to other nodes outside, the community was linked with other

329 communities.

330

331 **Figure 3.** Structural analysis of asparaptine A and *S*-(2-carboxy-*n*-propyl)-L-cysteine.

332 Left panel. Incorporation of ^{13}C to the asparagusyl moiety in asparaptine A. This non-labeled

333 asparaptine A was identified using an authentic standard compound [Level 1, the guideline of

334 Metabolomics Standards Initiative (MSI)]. Right panel. Incorporation of ^{13}C to the

335 2-carboxy-*n*-propyl moiety in *S*-(2-carboxy-*n*-propyl)-L-cysteine (Level 3, the guideline of

336 MSI). On the basis of paired ^{13}C -labeled and non-labeled MS/MS spectra, MS/MS spectra

337 were demonstrated using MassLyncs.

338

339 **Figure 4.** Structural analysis of asparaptines B and C.

340 In addition to using paired ^{13}C -labeled and non-labeled MS/MS spectra, a doubly labeled

341 MS/MS spectrum was employed for this analysis. Top. MS/MS spectrum of non-labeled

342 asparaptines B and C. Middle. MS/MS spectrum of asparaptines B and C labeled with ^{13}C

343 valine. Bottom. MS/MS spectrum of asparaptines B and C labeled with ^{13}C -labeled valine and

344 ^{13}C -labeled lysine/histidine. On the basis of paired ^{13}C -labeled and non-labeled MS/MS

345 spectra, MS/MS spectra were demonstrated using MassLyncs.

346

347 **Figure 5.** Effect of asparaptine A on hypertensive mice.

348 (a) Systolic blood pressure. (b) Diastolic blood pressure. (c) Heart rate. Blue line indicates the

349 water-fed group (control), and yellow line indicates the asparaptine A-fed group. Standard

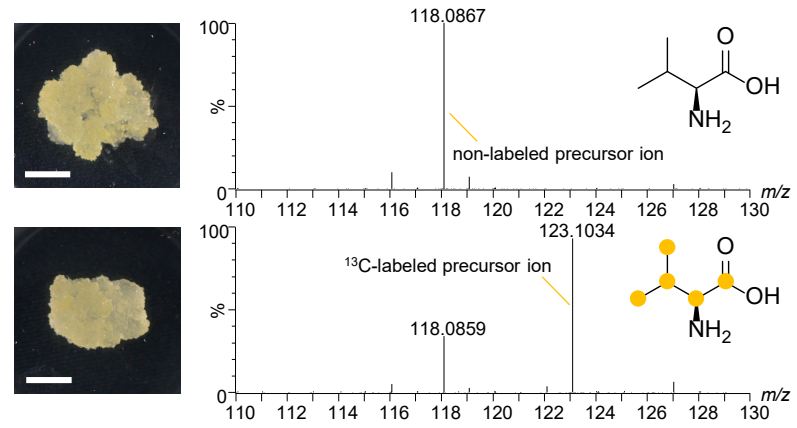
350 deviations (error bars) were calculated from the results of seven biological replicates. Asterisk

351 indicates significant differences between the groups at the annotated time point (Student *t*-test,

352 $p < 0.05$).

Figure 1

a



b

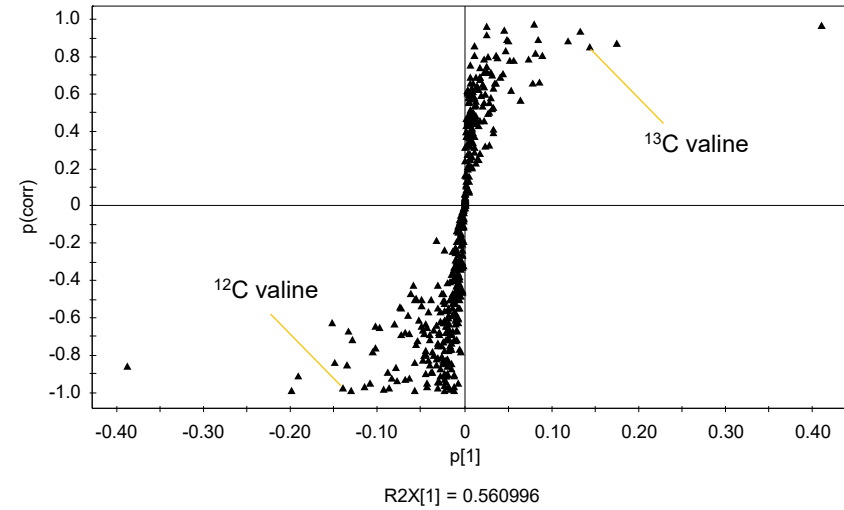


Figure 2

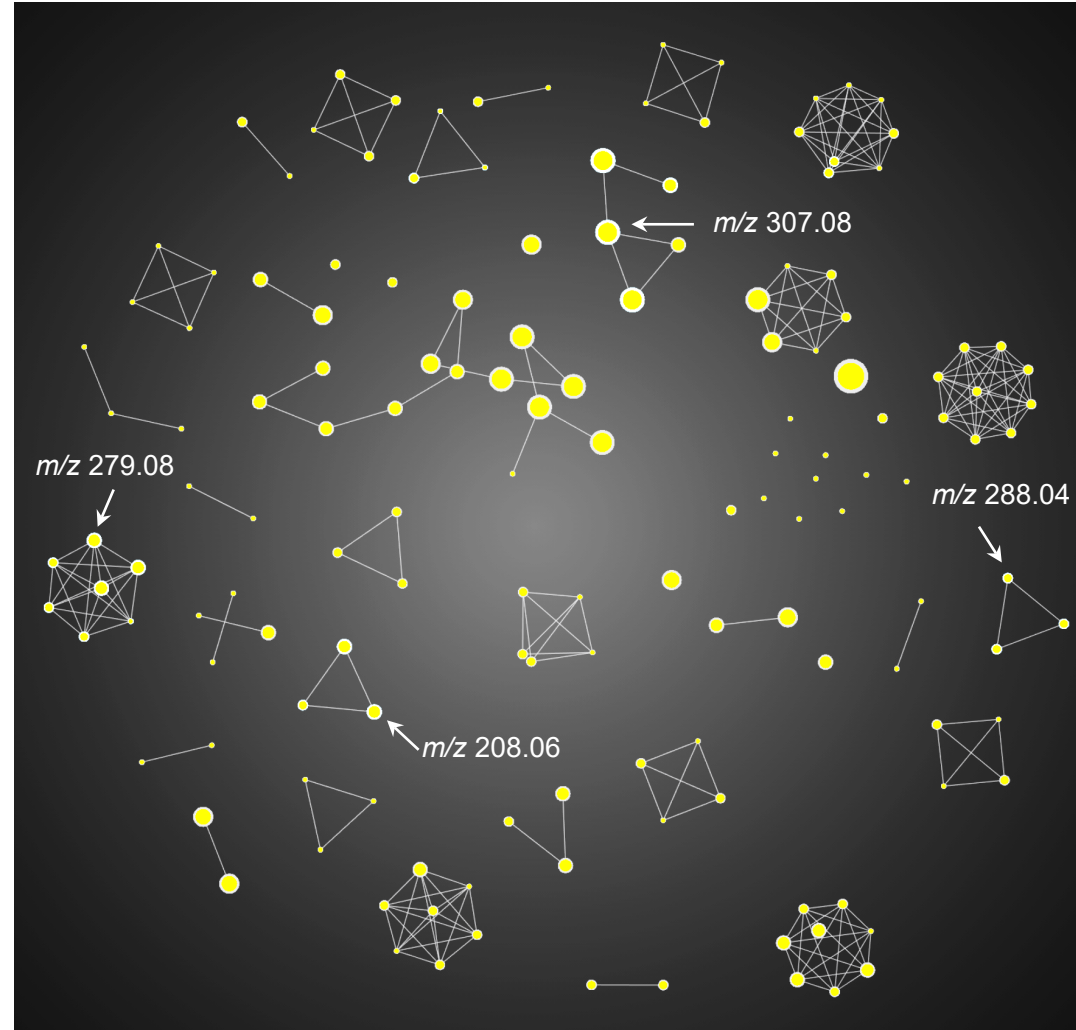
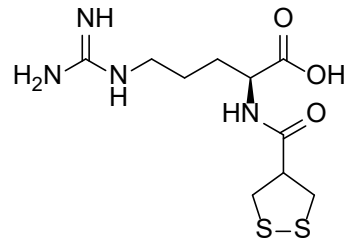
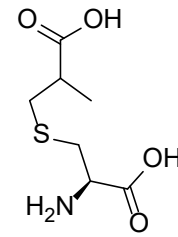
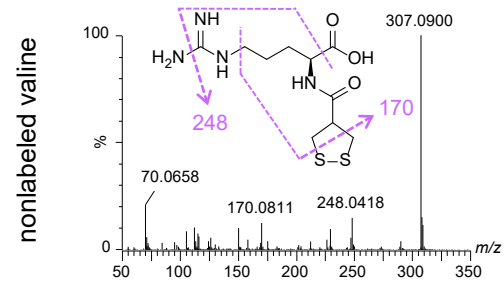


Figure 3



asparaptine A



S-(2-carboxy-*n*-propyl)-L-cysteine

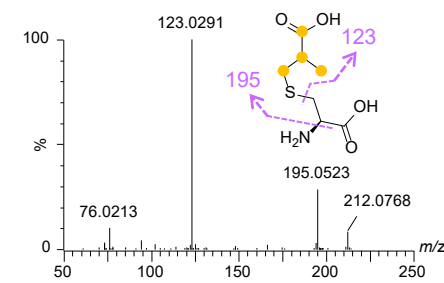
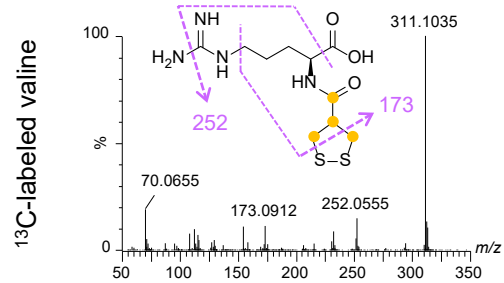
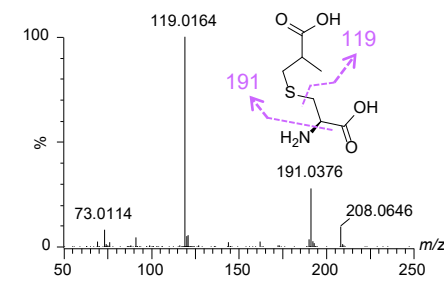
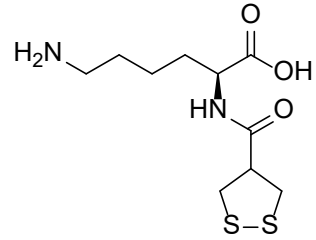
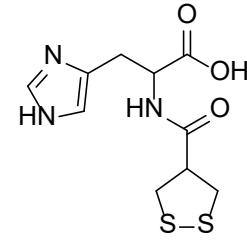
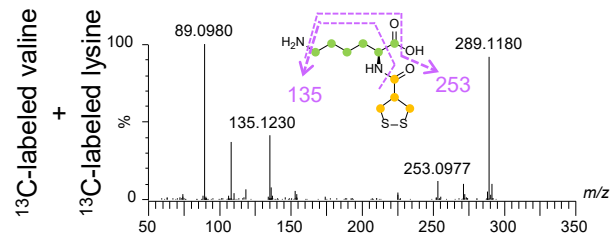
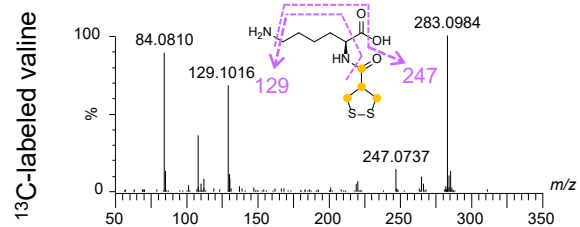
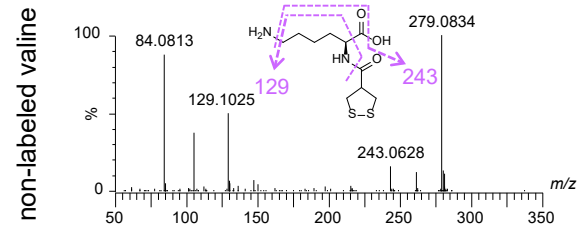


Figure 4



asparaptine B



asparaptine C

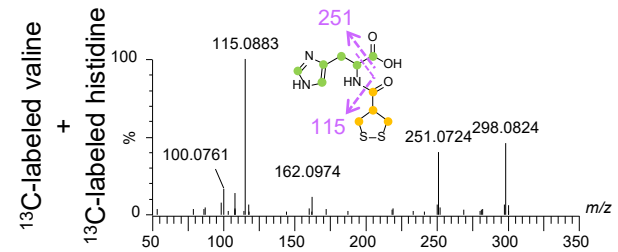
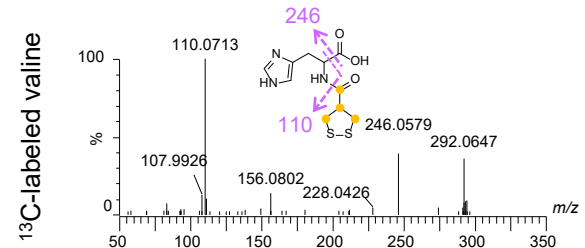
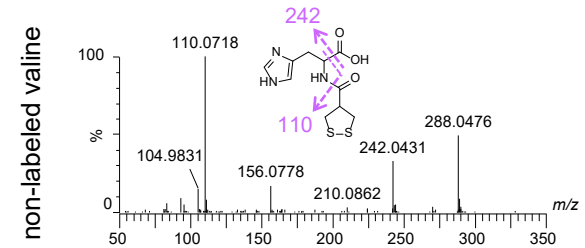


Figure 5

